# Interactions of Dynein Arms with B Subfibers of *Tetrahymena* Cilia: Quantitation of the Effects of Magnesium and Adenosine Triphosphate

DAVID R. MITCHELL and FRED D. WARNER

*Department of Biology, Biological Research Laboratories, Syracuse University, Syracuse, New York 13210. Dr. Mitchell's present address is the Department of Biology, Yale University, New Haven, Connecticut 06520.*

ABSTRACT *Tetrahymena* 30S dynein was extracted with 0.5 M KCl and tested for retention of several functional properties associated with its *in situ* force-generating capacity. The dynein fraction will rebind to extracted outer doublets in the presence of $Mg^{2+}$ to restore dynein arms. The arms attach at one end to the A subfiber and form bridges at the other end to the B subfiber of an adjacent doublet. Recombined arms retain an ATPase activity that remains coupled to potential generation of interdoublet sliding forces. To examine important aspects of the dynein-tubulin interaction that we presume are directly related to the dynein force-generating cross-bridge cycle, a simple and quantitative spectrophotometric assay was devised for monitoring the associations between isolated 30S dynein and the B subfiber. Utilizing this assay, the binding of dynein to B subfibers was found to be dependent upon divalent cations, saturating at 3 mM $Mg^{2+}$. Micromolar concentrations of $MgATP^{2-}$ cause the release of dynein from the B subfiber; however, not all of the dynein bound under these conditions is released by ATP. ATP-insensitive dynein binding results from dynein interactions with non-B-tubule sites on outer-doublet and central-pair microtubules and from ATP-insensitive binding to sites on the B subfiber. Vanadate over a wide concentration range ($10^{-6}$–$10^{-3}$ M) has no effect on the $Mg^{2+}$-induced binding of dynein or its release by $MgATP^{2-}$, and was used to inhibit secondary doublet disintegration in the suspensions. In the presence of 10 $\mu$M vanadate, dynein is maximally dissociated by $MgATP^{2-}$ concentrations $\geq 1$ $\mu$M with half-maximal release at 0.2 $\mu$M. These binding properties of isolated dynein arms closely resemble the cross-bridging behavior of *in situ* dynein arms reported previously, suggesting that quantitative studies such as those presented here may yield reliable information concerning the mechanism of force generation in dynein-microtubule motile systems. The results also suggest that vanadate may interact with an enzyme-product complex that has a low affinity for tubulin.

The motility of eukaryotic flagella and cilia is dependent upon the coordinated regulation of a basic sliding mechanism that is analogous to the sliding filament mechanism found in actin-myosin systems such as striated muscle. Elucidation of the sliding mechanism in cilia may have widespread importance because similar mechanisms may be involved in other microtubule-related phenomena such as axonal transport and mitosis.

By selective extraction and rebinding of ciliary components, it has been shown that the ATPase responsible for mechanochemistry resides in noncovalently attached projections or dynein arms which form two rows along the A subfiber of each outer-doublet microtubule (7, 9, 28). In the isolated form dynein arms occur as large complexes; *Tetrahymena* outer-arm dynein is commonly designated as 30S dynein from its apparent sedimentation coefficient (9). The inner row of arms may be



THE JOURNAL OF CELL BIOLOGY · VOLUME 87 OCTOBER 1980 84-97
 · 0021-9525/80/10/0084/14 $1.00

related to an ATPase activity that sediments at 14S (28), but 14S dynein has never been rebound to restore the inner row of arms; only the outer row has been unequivocally extracted and rebound (10, 28).

Arms projecting from the A subfiber of one outer doublet induce the translation of an adjacent doublet towards the tip of the axoneme (27). To generate sliding forces, the dynein arms must undergo a state transition coupled to the free energy released during ATP binding and hydrolysis. Warner (36) and Zanetti et al. (39) have shown that dynein arms *in situ* will attach to the B subfiber to form a stable cross-bridge between adjacent outer doublets. This attached state was apparently driven and maintained by divalent metal cations in the millimolar concentration range. A reduction in the percentage of bridged arms was seen in the presence of $MgATP^{2-}$, suggesting that substrate for the dynein ATPase might have a direct effect on the stability of the interaction. Takahashi and Tonomura (31) rebound isolated 30S dynein from *Tetrahymena* cilia to extracted doublet microtubules and found that 1 mM ATP dissociated the arms from the B subfiber, while arms attached to the A subfiber retained their doublet association. Similar qualitative reults have been obtained using isolated *Chlamydomonas* dynein and microtubules repolymerized from purified brain tubulin (13). The isolated dynein binds tightly to the neurotubules and forms ATP-sensitive intertubule cross-bridges, suggesting that opposite ends of the dynein arm complex form microtubule attachments that differ in their stability and in their sensitivity to added ATP.

Sea urchin dynein 1 (21S) will rebind to restore the beat frequency of extracted axonemes (7). Although *Tetrahymena* 30S dynein will also rebind to extracted outer doublets in the presence of $Mg^{2+}$ or $Ca^{2+}$ at millimolar concentrations, no restoration of normal function has been previously reported in the *Tetrahymena* system. We report here that *Tetrahymena* 30S dynein restores spontaneous microtubule sliding when it rebinds to extracted axonemes and we examine the nature of the interaction of dynein with the microtubules. To obtain quantitative data on dynein B subfiber interactions, we have developed a rapid and simple spectrophotometric dynein-microtubule binding assay. Using this assay, we have examined the dependence of dynein attachment upon $Mg^{2+}$ concentration and the sensitivity of dynein dissociation to $MgATP^{2-}$ concentration. Vanadate, an uncompetitive dynein ATPase inhibitor, has been used in several recent studies probing the mechanism of dynein mechanochemistry (11, 18, 26). Although vanadate inhibits microtubule sliding at low concentrations (26), we find that it has no effect on either the binding of dynein to doublet microtubules or dynein's dissociation by ATP. These results are discussed in terms of the specificity of dynein-microtubule interactions, the roles that these interactions may play in the force-generating cross-bridge cycle, and the mechanism of vanadate inhibition in this system.

## MATERIALS AND METHODS

### Isolation of Cilia

*Tetrahymena pyriformis* were grown in 1-liter low-form culture flasks in 2% proteose peptone, 0.2% glucose, 0.1% yeast extract. Cells were harvested by gentle centrifugation and resuspended in a small volume of culture medium. Dibucaine HCl was added from a 10-mM stock solution to give a final concentration of 1.5 mM, and deciliation was monitored by phase-contrast light microscopy. When deciliation was complete (1–2 min), the suspension was diluted with an equal volume of culture medium, transferred to centrifuge tubes, and spun at 4,000 rpm for 6 min in a Beckman JS 13 rotor (Beckman Instruments Inc., Spinco Div., Palo Alto, Calif.). The clear supernate containing the cilia was removed without disturbing the underlying layer of mucus, and was centrifuged at 10,000 rpm for 15 min. The pellet of cilia was resuspended in 5 mM $MgSO_4$, 0.5 mM EDTA, 100 mM KCl, 10 mM HEPES buffer, pH 7.4. Cilia were demembranated in 0.2% Triton X-100 containing the same buffer components, and the axonemes were collected by centrifugation through a 40% sucrose cushion at 8,000 rpm for 25 min.

### Doublet Microtubules

Outer doublets retaining their dynein arms were prepared by resuspending axonemes in 5 mM $MgSO_4$, 10 mM HEPES, pH 7.4, and adding 20 $\mu$M ATP to induce sliding disintegration (38). The extent of disintegration was monitored by phase-contrast microscopy and by following the drop in absorbance at 350 nm ($A$ 350 nm). Under these conditions, 80–90% of the axonemes disintegrate, causing a 25–35% drop in $A$ 350 nm. Preparations with less than a 25% drop in $A$ 350 were not used. Doublets were washed in 0.5 mM EDTA, 10 mM HEPES, pH 7.4, and resuspended in various test solutions (see Results).

### Extracted Axonemes

An outer-doublet fraction retaining inter-doublet or nexin links but lacking dynein arms was prepared by the method of Gibbons (9): whole axonemes were dialyzed against 1 mM HEPES, 0.01 mM EDTA, pH 7.4, for 14 h and collected by centrifugation to separate extracted axonemes from the soluble components. The ratio of sample volume to dialysate was 1:400 and the dialysate was changed after the first 4 h.

### Dynein Isolation

Axonemes were resuspended in 0.55 M KCl, 5 mM $MgSO_4$, 0.1 mM EDTA, 10 mM HEPES, pH 7.4, for 20 min at 0°C and centrifuged at 50,000 $g$ for 30 min. The supernate was dialyzed against 0.5 mM EDTA, 10 mM HEPES, pH 7.4, clarified by centrifugation at 50,000 $g$ for 30 min, and concentrated to 0.5–1.0 mg/ml on an Amicon PM30 ultrafiltration membrane (Amicon Corp., Scientific Sys. Div., Lexington, Mass.). For some experiments, this crude dynein preparation was subjected to further fractionation on a 0–30% sucrose gradient spun at 35,000 rpm for 15 h in a Beckman SW40 rotor.

### Dynein-binding Assays

For turbidimetric assays, optical absorption at $A$ 350 was monitored continuously before and after the addition of dynein (experimental) or an equal volume of buffer (control) to a preparation of microtubules suspended in a test solution of variable ionic composition. The total assay volume was 0.5 ml. Microtubule preparations were adjusted to an $A$ 350 nm = 0.200 (60–80 $\mu$g protein/ml) and 10–20 $\mu$g of dynein was added, sufficient to raise the $A$ 350 nm by 50% in the presence of 6 mM $Mg^{2+}$. The effects of $MgATP^{2-}$ were examined by adding 5 $\mu$l of concentrated stock solutions to both experimental and control preparations and measuring the drop in $A$ 350 nm.

For direct measurements of protein binding, experimental preparations were transferred to centrifuge tubes and layered over 40% sucrose, 10 mM HEPES, 0.01 mM EDTA, and $MgSO_4$ concentrations identical to those of the test solution. Preparations were spun at 40,000 rpm in an SW40 rotor for 15 min to remove the microtubules from the applied sample. The amount of protein and ATPase activity in the supernate was tested after centrifugation and the difference between these values and controls was used as a measure of the amount of protein bound to the tubules. Control preparations contained dynein but no microtubules.

### ATPase Assay

Vanadate-free $Na_2ATP$ was purchased from Sigma Chemical Co. (St. Louis, Mo.). Sodium meta-vanadate ($Na_2VO_3 \cdot nH_2O$) was purchased from Fisher Scientific Co. (Pittsburgh, Pa.) and was prepared assuming a stoichiometry of 2 $H_2O/VO_3$ as reported by Kobayashi et al. (18). Using this assumption, we have obtained results on the inhibition of *Tetrahymena* 30S dynein comparable to those reported by Kobayashi et al. (18).

ATPase assays were performed in 40 mM HEPES, 6 mM $MgSO_4$, 0.1 mM EDTA, pH 7.4, at 15°C. Dynein was preincubated in the assay solution for 5 min and the reaction was started by the addition of ATP. Aliquots were removed at several time intervals and the reaction was stopped by the addition of TCA (final concentration 10%). The inorganic phosphate released was measured by the method of Taussky and Shorr (33) and the activity estimated from the region of linear phosphate release.

## Protein Concentration

Protein concentrations were estimated by the Coomassie Blue dye binding method of Bradford (3) and with bovine serum albumin as standard.

## Electron Microscopy

Samples were prepared for thin-section electron microscopy by fixation in 1% glutaraldehyde, 6 mM $MgSO_4$, 40 mM HEPES, pH 7.4, for 30 min, rinsed for 5 min in buffer, and postfixed in 1% $OsO_4$ (same buffer components). Dehydration was done in a graded ethanol series followed by embedding in Epon 812. Thin sections were stained in 4% aqueous uranyl acetate for 15 min followed by staining in Reynolds' lead citrate for 3 min. Negatively contrasted specimens were stained with 4% aqueous uranyl acetate. All specimens were examined in a Siemens 101 electron microscope operated at 80 kV.

# RESULTS

## Reassociation of Dynein with Extracted Axonemes

Dynein was extracted from *Tetrahymena* axonemes with 0.55 M KCl as described in Materials and Methods. Fractionation of this dynein preparation on a 0–30% sucrose gradient reults in one major and two minor protein peaks (Fig. 1). The major peak sediments at 25S–30S and is labeled 30S dynein in accordance with the results of Gibbons (10). When each peak was tested separately for its ability to recombine with extracted axonemes, all of the binding properties resided in the 30S protein; protein from the other peaks neither rebound nor had any effect on the binding of the 30S fraction under the conditions examined.

Several investigators have previously shown that *Tetrahymena* 30S dynein will reattach to outer doublets in the presence of $Mg^{2+}$, restoring the dynein arm structure to its normal position (9, 25, 28, 31). Extensive low ionic strength dialysis of *Tetrahymena* cilia appears to have completely removed both inner and outer rows of dynein arms, as well as central-pair tubules (Fig. 2 *a*). The subsequent addition of ATP to extracted axonemes does not result in active disintegration of the axonemes when potential disintegration is monitored by either negative contrast electron microscopy or A 350 nm (38), thus confirming the complete removal of both rows of arms. Fig. 2 *b* shows the results of adding KCl extracted 30S *Tetrahymena* dynein to dialysis-extracted outer doublets in the presence of 6 mM $Mg^{2+}$. The readded arms not only rebind to the A subfibers but form bridges to the B subfibers as well. The addition of $MgATP^{2-}$ to recombined axonemes results in disintegration of the axonemes caused by microtubule sliding (Fig. 2 *c*). The rebound arms thus retain both ATPase activity and the mechanochemical coupling necessary to convert the energy released by hydrolysis into motion.

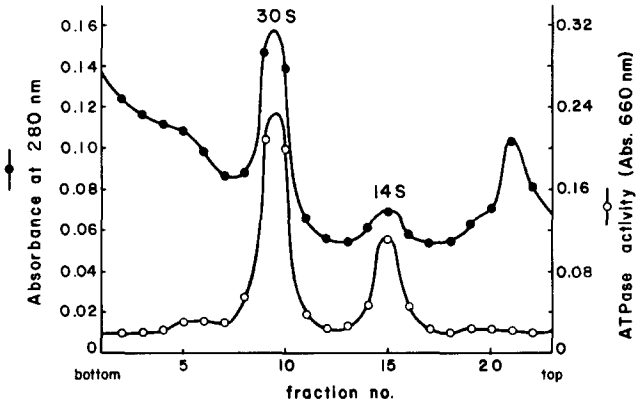


FIGURE 1 Fraction profile of KCl-extracted dynein centrifuged in a 0–30% sucrose gradient containing 0.01 mM EDTA, 10 mM HEPES, pH 7.4. 20-drop fractions were collected from the bottom of the tube and monitored for protein concentration (●) and ATPase activity (○). The two peaks of activity are labeled 30S and 14S according to the sedimentation coefficients reported by Gibbons (10).

The lower portion of Fig. 2 is a record of the changes in turbidity that accompany the consecutive additions of dynein and ATP to a suspension of extracted axonemes. Dynein addition causes an immediate increase in turbidity, measured as the *A* 350 nm, which levels off after 10–20 min. This increase in *A* 350 nm is dependent upon the presence of $Mg^{2+}$ in the millimolar concentration range and was used as the basis for a quantitative dynein binding assay described below. An ATP-dependent decrease in *A* 350 nm results from disintegration of the axonemes, as previously described by our laboratory (38, 39). No turbidity changes occur when ATP is added to extracted axonemes in the absence of dynein or $Mg^{2+}$.

## $Mg^{2+}$ Dependency of Dynein Binding to Doublet Microtubules

To examine the interaction of isolated dynein with the B subfiber, a suspension of individual doublets was prepared by exposing whole axonemes to 20 μM $MgATP^{2-}$ (Fig. 3). Doublets prepared in this manner retain their normal complement of dynein arms on the A subfiber. Fig. 4 shows the appearance of doublets that were negatively stained before and after the addition of isolated 30S dynein in the presence of 6 mM $Mg^{2+}$. The added dynein has bound to the B subfiber to create a row of projections with the same periodicity (24 nm) as the A-subfiber arms. As described previously (31), arms on both the A and B subfiber tilt toward the base of the axoneme.

The absorbance trace seen in Fig. 4 records the increase in *A* 350 nm seen when dynein (10 μg/ml) was added to doublets (40 μg/ml) in the presence of 6 mM $MgSO_4$. The extent of the increase in *A* 350 nm was dependent upon the $Mg^{2+}$ concentration between 0 and 3 mM $Mg^{2+}$, with little absorbance increase seen in the absence of $Mg^{2+}$. To determine the relationship between these absorbance changes and the amount of dynein bound to the doublets, samples were centrifuged to remove doublets and the amount of unbound dynein remaining in the supernatant fraction was measured at several different $MgSO_4$ concentrations. In Fig. 5 the mean values from duplicate assays are plotted. The absorbance increases are directly proportional to the amount of protein (Fig. 5, top) and ATPase activity (Fig. 5, bottom) bound to the doublets. Although the slope of the line relating protein binding to *A* 350 nm was somewhat variable from preparation to preparation, the relationship was consistently linear and highly reproducible within each preparation of doublets and dynein over the range of protein concentrations examined.

The $Mg^{2+}$ dependence of dynein binding to the B subfiber is plotted in Fig. 6 using both *A* 350 nm and direct protein measurements. The results have been normalized for purposes of comparison between methods and different dynein and doublet preparations, by making the largest result obtained equal to 100%. The bridging frequencies of *in situ* dynein arms seen by thin-section electron microscopy and reported by Zanetti et al. (39) are also included in Fig. 6 for comparative purposes. The three methods clearly show that the dynein-B-subfiber association is strictly dependent upon the $Mg^{2+}$ con-

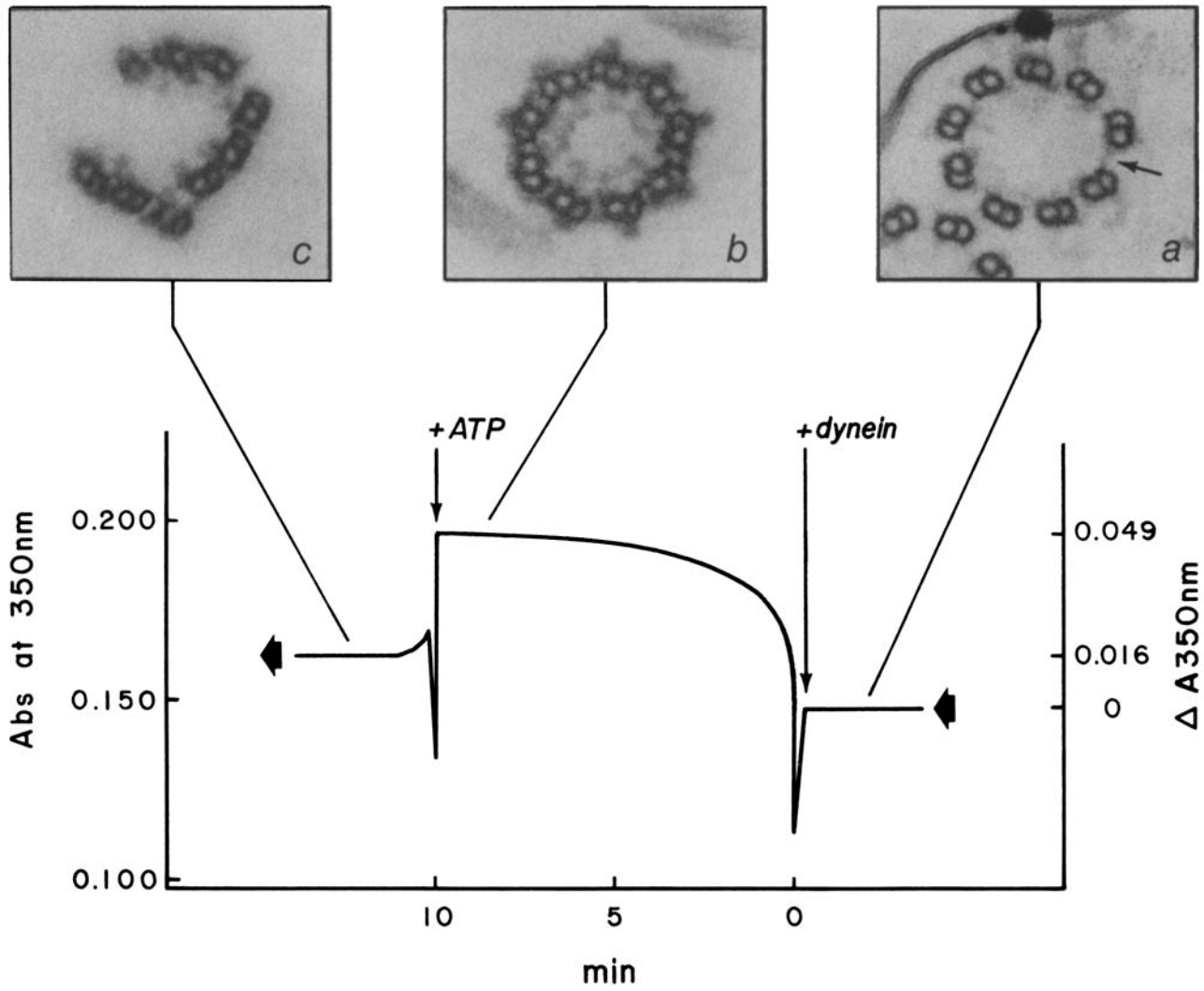


FIGURE 2 Lower panel: Absorbance tracing at 350 nm of outer-doublet fraction. Dynein was added at the first arrow ($t = 0$) and 20 $\mu$M ATP at the second arrow ($t = 10$). The binding of dynein to the axoneme is accompanied by an increase in A 350 nm which levels off within 5–10 min. The drop in A 350 nm after ATP addition reflects axonemal disintegration. Upper panel: Electron micrographs of axonemes extracted by low ionic strength dialysis and fixed in 6 mM $MgSO_4$, 40 mM HEPES, 1% glutaraldehyde, pH 7.4, and corresponding to the three regions of the absorbance tracing. (*a*) Before addition of dynein, no arms project from outer doublets although adjacent doublets remain connected by nexin links (arrow). (*b*) After dynein addition, arms have reattached and form bridges between adjacent doublets. (*c*) Addition of 0.1 mM ATP has induced disintegration of the axonemes. × 135,000.

centration, saturating at ~3 mM $Mg^{2+}$. Even though care was taken to exclude divalent cations from all solution components, some dynein (20 ± 12% of the maximum; $n = 5$) bound in the absence of added $Mg^{2+}$. This nonspecific binding may simply reflect an inability to completely remove bound $Mg^{2+}$ or $Ca^{2+}$ from the proteins, or it may result from binding to abnormal sites as discussed below in "Specificity of Dynein Binding."

## *Effects of ATP on $Mg^{2+}$-dependent Dynein Binding*

The release of dynein arms from the B subfiber by ATP may represent an important step in the mechanochemical cross-bridging cycle of dynein arms. This ATP effect has been examined by both thin-section and negative-stain electron microscopy (31, 36). Thin-section electron microscopy, while producing quantitative data, provides only a static picture of a dynamic process and is further limited in its ability to examine the effects of ATP by the fact that ATP hydrolysis may continue during the fixation process, lowering the effective substrate concentration at the time of arm immobilization. Negative-stain electron microscopy, on the other hand, can provide only qualitative information on dynein attachment and release because the negative-stain procedure itself often causes considerable disruption of dynein-tubule associations.

To obtain reliable quantitative data on the dissociation of dynein from B subfibers, the effect of ATP on doublets decorated with dynein was followed turbidimetrically. A previous study in which ATP-induced decreases in turbidity were equated with the dissociation of dynein (31) may have actually recorded the drop in turbidity that accompanies the disintegration of trypsin-digested axonemes (26, 30, 38) rather than that caused by dynein release (see Discussion).

The effect of adding 20 $\mu$M ATP to decorated doublets in 6 mM $MgSO_4$ as seen by electron microscopy is illustrated in Fig. 7. Most of the dynein arms have been dissociated from the B subfiber by this treatment while A-subfiber arms retain their normal periodic association. Addition of ATP also causes a

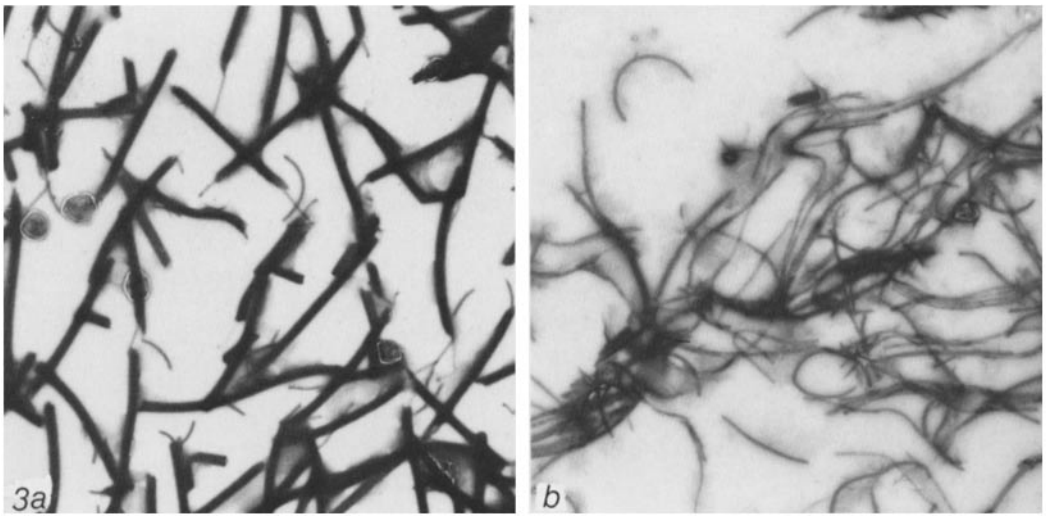


FIGURE 3 Whole axonemes negatively contrasted with uranyl acetate (*a*) before and (*b*) after addition of 20 μM ATP. Ancillary conditions, 5 mM $MgSO_4$, 0.4 mM EDTA, 0.1 M KCl, 10 mM HEPES, pH 7.4. The addition of ATP has caused the axonemes to undergo active sliding disintegration into individual doublets and groups of doublets. × 5,000.

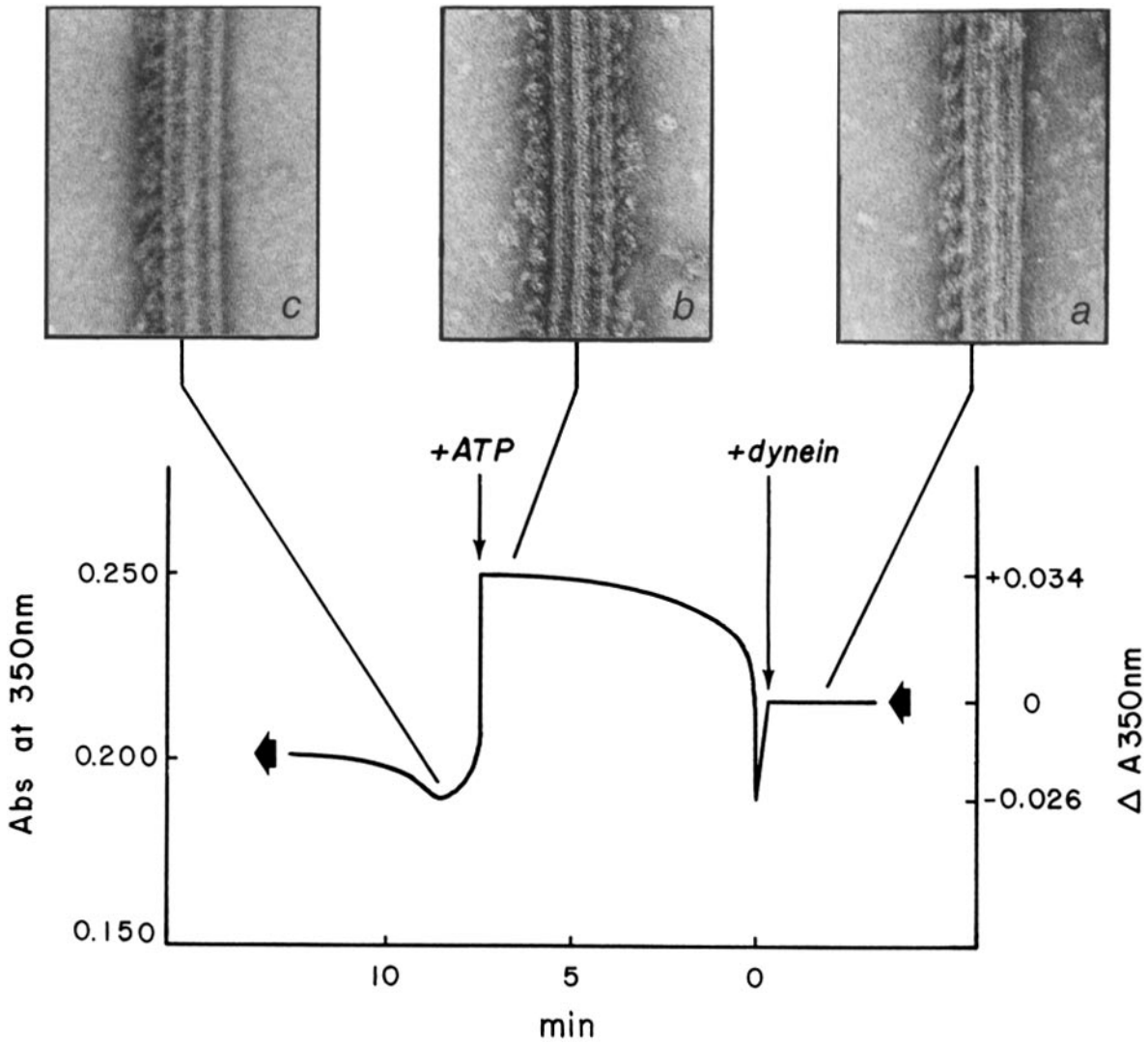


FIGURE 4 Lower panel: Absorbance tracing showing changes in *A* 350 nm of a suspension of unextracted doublets after additions of dynein (first arrow) and ATP (second arrow). The absorbance changes after ATP addition result from a combination of several effects (see text). Upper panel: electron micrographs of unextracted doublet microtubules corresponding to the three regions of the absorbance tracing. (*a*) Before dynein addition, arms project only from the A subfiber. (*b*) After the addition of dynein, arms project from both the A and B subfibers. (*c*) The addition of 20 μM ATP results in loss of arms from the B subfiber. × 182,000.

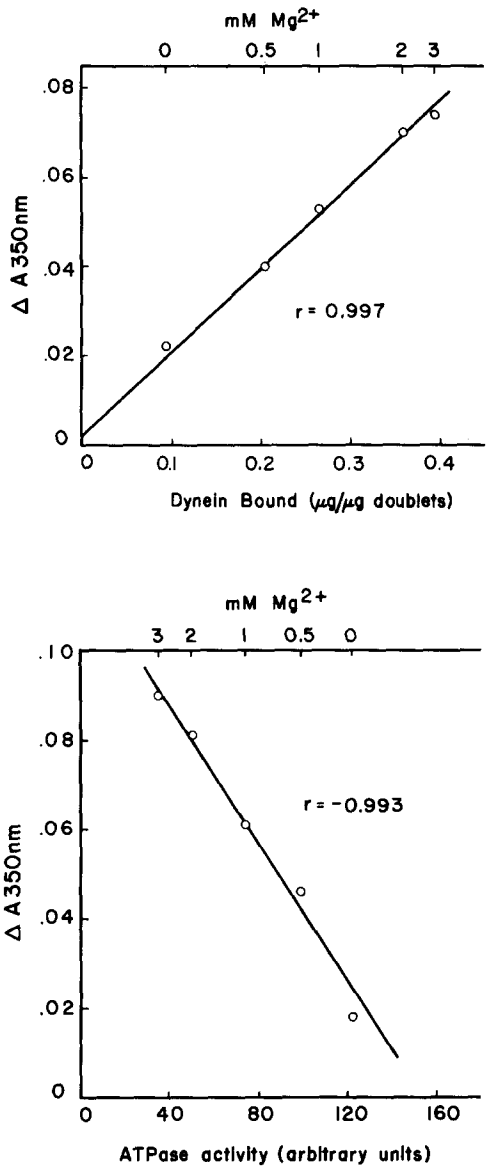


FIGURE 5 The graphs depict the relationship between the increase in *A* 350 nm and the amount of dynein bound to doublets in varying concentrations of $MgSO_4$. Final concentrations were 40 μg/ml dynein and 70 μg/ml doublets. The amount of dynein bound was measured either as the amount of protein sedimenting with the doublets (top) or was estimated from the ATPase activity remaining in the supernate after the doublets were removed by centrifugation (bottom). Using either method, the correlation coefficients (*r*) show that *A* 350 nm increases linearly with the amount of dynein bound.

decrease in *A* 350 nm of a suspension of decorated doublets as seen in the lower portion of Fig. 4. This response is characterized by an immediate drop in absorbance, which stabilizes within 1–2 min, but gradually begins to increase again. We have not examined this part of the response in detail, but it is seen only at low ATP concentrations and may be caused by the rebinding of dynein after hydrolysis as suggested by Takahashi and Tonomura (31). The initial decrease in *A* 350 nm is caused by the additive effects of two separate phenomena and can therefore be broken into two separate components. When doublet microtubules retaining A-subfiber arms are resuspended in the presence of $Mg^{2+}$, they reassociate with each other through $Mg^{2+}$-induced dynein cross-bridges (Fig. 7*a*; cf. reference 13). The subsequent addition of ATP causes disaggregation as the doublets undergo a secondary disintegration and *A* 350 nm decreases (Fig. 8, top). If isolated dynein has been bound to the doublets, ATP induces dissociation of that dynein from the B subfiber as well as secondary disintegration, and both phenomena presumably contribute to the decrease in *A* 350 nm. Fig. 8, bottom shows the absorbance change caused only by dynein release, calculated by subtracting the portion caused by sliding. ATP appears to have a half-maximal effect on dynein release at a concentration of 5μM, with no further effects occurring above 10 μM. As an important check on the reliability of this method for quantitating the effects of ATP, an alternative procedure was used which eliminates the contribution of sliding to the absorbance decrease by inhibiting sliding, but not dynein release (see below).

## *Effects of Vanadate on Mechanochemistry and on Dynein-Tubule Interactions*

Vanadate is an uncompetitive inhibitor of dynein ATPase activity (11, 18). It also lowers the beat frequency of reactivated flagella (11) and inhibits sliding disintegration of trypsin-treated sea urchin sperm axonemes (26). On the other hand, vanadate does not inhibit several phenomena which are thought to result from the ATP-induced release of dynein arms. It has no effect on the relaxation of rigor-wave sperm by $MgATP^{2-}$ (8) or on the ability of ATP to decrease the stiffness of demembranated sperm axonemes (21). We therefore tested the effects of vanadate with the expectation that it might inhibit the secondary sliding of doublets without interfering in the binding and release of dynein.

The sliding disintegration of whole *Tetrahymena* axonemes is readily inhibited by vanadate (Fig. 9). ATP was added to whole axonemes and sliding was monitored by measuring the decrease in *A* 350 nm. Sliding is over 90% inhibited by 5 μM vanadate whether sliding is induced by 30 μM ATP (an optimal concentration under these conditions; 38) or 100 μM ATP. To see whether vanadate interfered with dynein binding to the B

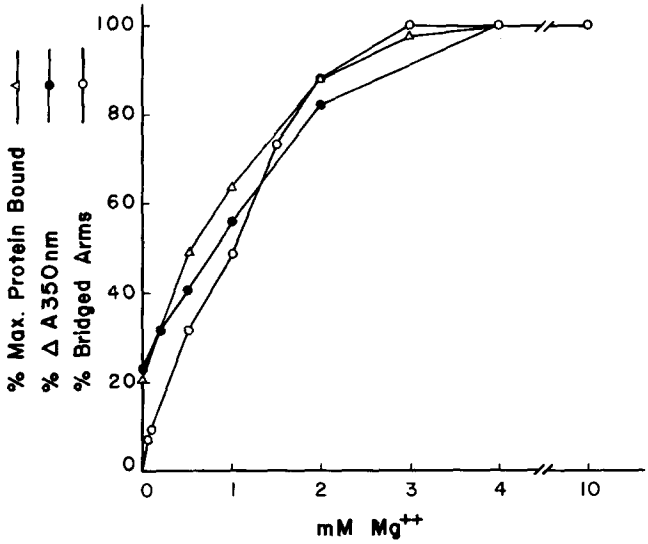


FIGURE 6 Plot showing the dependence of dynein binding upon $MgSO_4$ concentration; (Δ) protein bound to the doublets; (●) increase in *A* 350 nm caused by dynein addition; (○) percentage of dynein arms forming cross-bridges in whole axonemes (from reference 39). Binding of isolated dynein to the B subfiber clearly follows the same $Mg^{2+}$ dependence as *in situ* bridging of dynein arms to B subfibers.

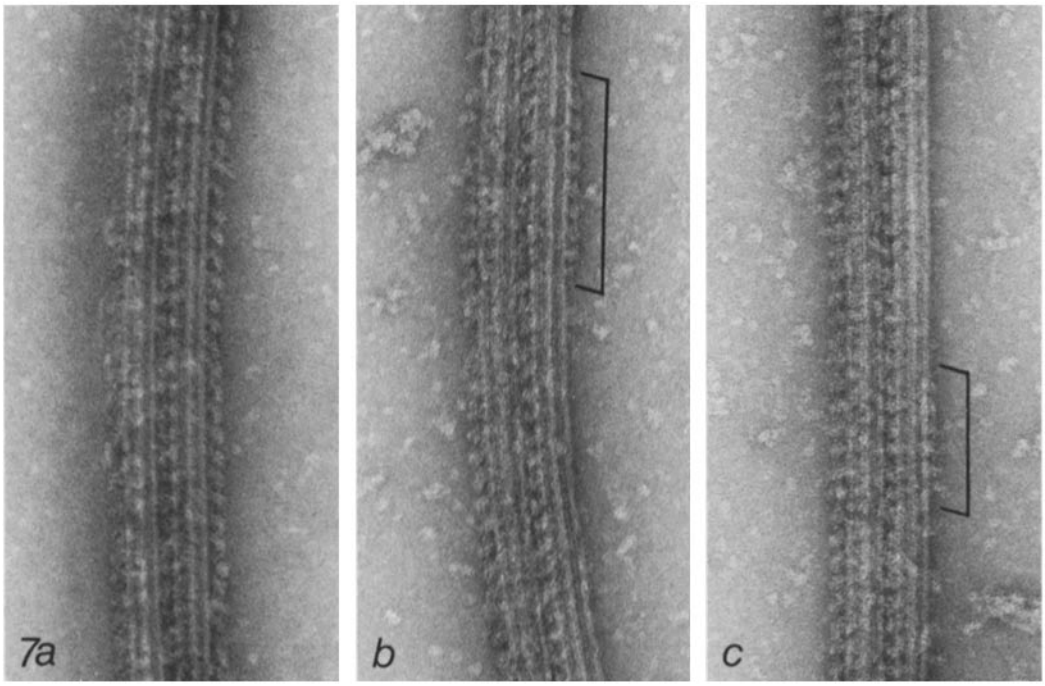


FIGURE 7 Electron micrographs of unextracted doublets decorated with dynein in 6 mM $MgSO_4$. (*a*) Before ATP addition, B subfibers are uniformly decorated with dynein arms having a 24-nm repeat period and tilting toward the base of the axoneme. Addition of 20 $\mu$M ATP (*b* and *c*) results in considerable loss of dynein from the B subfiber, although some patches of decoration remain (brackets). × 120,000.

subfiber, doublets were preincubated with vanadate at several concentrations and *A* 350 nm was recorded before and after adding dynein (Fig. 10, left). The difference between these two measurements (Fig. 10, right) gives a relative indication of the amount of dynein bound. It is clear that vanadate concentrations between $10^{-6}$ and $10^{-3}$ M do not inhibit dynein binding. The increase in *A* 350 nm seen at vanadate concentrations $>10^{-4}$ M is caused by the formation of a polyanionic vanadate species (17) and does not reflect changes in the turbidity of the doublet suspension.

The effects of vanadate on ATP-induced dynein release were examined in a similar manner (Fig. 11). Vanadate effectively inhibits the sliding seen when 100 $\mu$M ATP is added to doublets alone but it has no effect on the release of dynein from decorated doublets even at vanadate concentrations as high as 1 mM. Therefore, by the use of 10 $\mu$M vanadate to inhibit sliding, the dependence of dynein dissociation upon ATP concentration was retested. In the presence of 6 mM $MgSO_4$ and 10 $\mu$M vanadate, ATP has a half-maximal effect at 0.2 $\mu$M and a maximal effect at 1 $\mu$M (Fig. 12). This concentration is considerably lower than that required for a half-maximal effect in the absence of vanadate (5 $\mu$M, Fig. 8, bottom). Such a decrease in the apparent half-maximal substrate concentration is consistent with the uncompetitive nature of vanadate inhibition (see Discussion).

## Specificity of Dynein Binding

From the results presented in Fig. 12, it is clear that a significant amount of the dynein that binds in 6 mM $Mg^{2+}$ is not released by ATP. The ATP concentrations that produced maximal and half-maximal release varied little among preparations, whereas the maximal percent released varied considerably. 37 ± 10% ($n$ = 5) of the dynein remained bound even at nucleotide concentrations up to 1 mM. This indicates the presence of two classes of dynein-tubule interactions, one which remains stable in the presence of $MgATP^{2-}$ and one which does not. The relative contributions of these two classes vary somewhat from one preparation to the next, for reasons that remain unclear. Only ATP-sensitive binding to B-subfiber sites should be occurring if dynein binding is limited to the types of dynein-tubule interactions that occur *in situ*. A number of possible reasons for ATP-insensitive dynein binding to unextracted doublets have been examined in an attempt to account for these observations.

During preparation, doublets may lose a small fraction of dynein into solution, thus exposing A-subfiber binding sites and permitting ATP-insensitive dynein binding. Tests of the amount of dynein released into solution show that <2% of the protein that can be extracted by KCl is released during the course of doublet preparation. Binding to A-subfiber sites exposed in this manner cannot contribute significantly to ATP-insensitive dynein binding by outer doublets. As seen in Fig. 7, not all of the dynein that binds to B subfibers is released at saturating ATP concentrations. Clear morphological criteria do not exist for distinguishing dynein arm polarity in negatively stained preparations. It is possible that the proximal (A-subfiber) end of the arm could interact with B-subfiber sites, which might result in an ATP-insensitive attachment to the B subfiber. Of those arms that are attached in an ATP-sensitive manner, the percentage that remain attached at saturating ATP concentrations depends upon the equilibrium constant for the interaction between B-subfiber tubulin sites and the enzyme-substrate or enzyme-product complex that predominates under these conditions. Because these parameters are not easily estimated in the absence of detailed information on dynein enzyme kinetics, their contribution to the observed phenomena cannot be assessed.

Isolated *Chlamydomonas* dynein will form bridges between single microtubules repolymerized from brain tubulin (13).

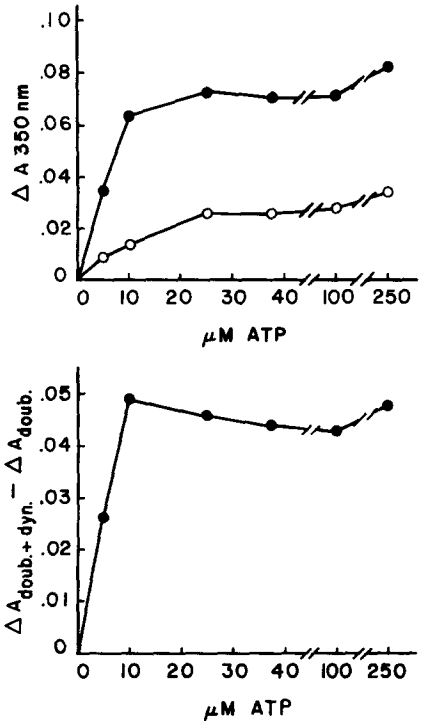


FIGURE 8 Top: Plot of the decrease in *A* 350 nm seen when varying ATP concentrations are added either to a suspension of unextracted doublets (O), or to unextracted doublets plus dynein (●). For doublets alone, each point is the difference between the absorbance before and after adding ATP to the doublet suspension, and measures a residual component of microtubule sliding. For doublets plus dynein, each point is the difference between the maximum absorbance after dynein addition and the minimum absorbance after adding ATP, measured from traces similar to the lower panel of Fig. 4. This indicates both residual sliding and the dissociation of dynein from the B subfiber. Bottom: The difference between each pair of points in the top graph has been plotted to show only that portion of the absorbance change that is caused by dynein dissociation. ATP appears to have a half-maximal effect on dynein dissociation at a concentration of ~5 μM.

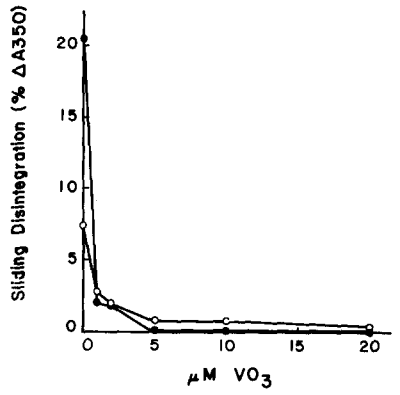


FIGURE 9 The graph depicts the effects of vanadate on the sliding disintegration of whole axonemes. Axonemes were preincubated in 5 mM $MgSO_4$, 10 mM HEPES, pH 7.4, and varying concentrations of vanadate for 5 min before the addition of 30 μM (●) or 100 μM (O) ATP. 5 μM vanadate inhibits sliding disintegration by over 95%.

When ATP is added, the microtubules are no longer cross-linked and the dynein arms retain their association with only one of the two tubules. This shows that dynein is capable of forming ATP-sensitive and ATP-insensitive attachments to neurotubules, and indicates that dynein can interact directly with tubulin. Specific binding sites such as may occur on the A and B subfibers of outer-doublet microtubules either are not required for dynein binding or are present in other types of microtubules as well. This raises the possibility that dynein could attach to many nonspecific sites on doublet tubules, resulting in an ATP-insensitive dynein component.

The specificity of dynein binding to outer doublets was examined by fixing decorated doublets for thin-section microscopy in the presence of 6 mM $MgSO_4$. Fig. 13 shows that isolated dynein can cross-link doublet microtubules in many atypical orientations. Arms can apparently interact with many sites on the tubulin lattice and hence project from several positions. Similar dynein attachment has been reported when dynein was added in stoichiometric excess to extracted axonemes (28) and can be seen in Fig. 4b. Flocculent material and armlike projections adhere to the periphery of the axoneme, especially at the junction between the A and B subfibers. Atypical dynein binding can also be observed in negatively stained preparations. Dynein arms are not normally found on the A-subfiber tip beyond the termination of the B subfiber (Fig. 14*a*). After the addition of dynein, this region of the A

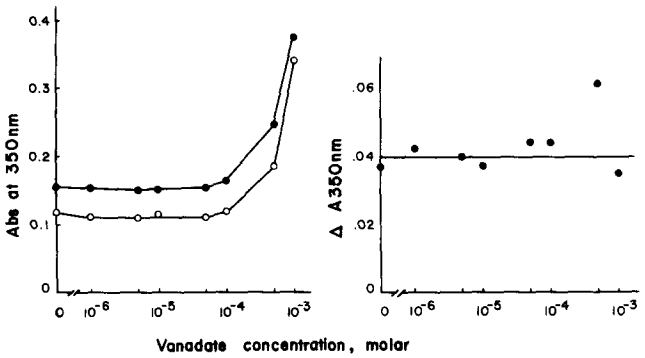


FIGURE 10 The graphs depict the effects of vanadate on the binding of dynein to unextracted doublets in 6 mM $MgSO_4$, 10 mM HEPES, 0.1 mM EDTA, pH 7.4. Left: *A* 350 nm of doublets before (O) and after (●) addition of a constant amount of dynein. Right: Difference between each pair of data points showing the increase in *A* 350 nm caused by dynein binding. Vandate has no effect on attachment of dynein to the B subfiber. The increase in *A* 350 nm above $10^{-4}$ M vanadate is caused by the formation of metavanadate complexes.

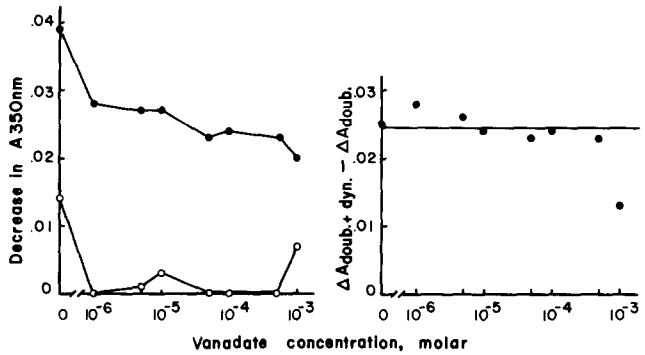


FIGURE 11 The graphs depict the effects of vanadate on the release of dynein by 100 μM ATP. The conditions are the same as in Fig. 10. Left: Decrease in *A* 350 nm when ATP is added to doublets (O) or doublets plus dynein (●). Right: Plot of the difference between each pair of data points indicating the absorbance drop caused by dynein dissociation. Vanadate does not effect dynein dissocation under these conditions.

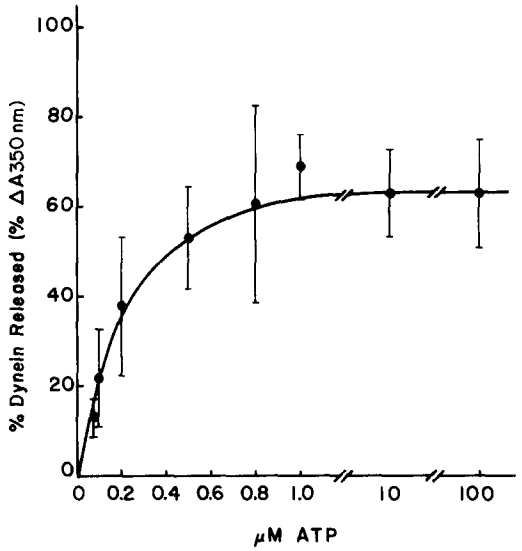


FIGURE 12 The effects of ATP concentration on dynein dissociation in the presence of 10 μM vanadate. Ancillary conditions are as described in Fig. 10. Ordinate values represent the percentage of the increase in A 350 nm caused by dynein binding that is lost upon ATP addition. Each point is the mean of values from five separate experiments. ATP releases ~60% of the bound dynein and has a half-maximal effect at ~0.2 μM. Error bars indicate the standard deviation.

subfiber is decorated with arm structures (Fig. 14*b*). When dynein is added in a large stoichiometric excess, both A and B subfibers become completely covered by rows of arms, giving the doublet a cross-hatched appearance (24 nm) (Fig. 15). This periodicity may be related to some feature of the underlying periodicity of the helical tubulin lattice (1).

The interaction of isolated dynein with A-subfiber sites was examined by adding dynein to doublets that had been extracted with 0.55 M KCl. When dynein was mixed with extracted doublets in the presence of 6 mM $MgSO_4$ only 30% of the dynein-dependent increase in *A* 350 nm was lost upon ATP addition (Table I). However, when dynein was added to unextracted doublets at the same dynein:tubule stoichiometry, 70% of the absorbance increase was ATP-sensitive. In both cases the same final absorbance was reached, regardless of the order of addition of ATP and dynein. This indicates that when both A- and B-subfiber sites are available, dynein binds preferentially in an ATP-insensitive fashion. But when only B-subfiber sites are exposed, dynein binding is predominantly ATP-sensitive.

In addition to binding to the A and B subfibers of outer doublets, dynein arms bind to central-pair microtubules (Figs. 16 and 17). Because most of the length of the central pair is covered with its own unique set of projections, dynein can only bind to the projection-free segment near the axonemal tip (Fig. 16*b*, *c*, and *e*), or to regions where the sheath projections have come off the tubules (Figs. 16*d* and 17*b*). Arms attached to the central pair have the same morphology, periodicity, and orientation as arms attached to the A subfiber, and appear to remain attached after ATP is added.

These atypical modes of binding, while difficult to quantitate, could account for most, if not all, of the ATP-insensitive fraction of bound dynein seen in Fig. 12. Binding to atypical sites on doublets probably accounts for the greatest proportion, with lesser contributions from central-pair decoration and replacement of arms lost from the A tubule during preparation.

It should be noted that what we term atypical dynein binding may, in fact, represent normal dynein binding properties of microtubules. Our results and those of Haimo et al. (13) suggest that ATP-insensitive and ATP-sensitive classes of dynein binding sites may be intrinsic properties of the tubulin dimer lattice. Binding site specificity required by the highly ordered functional geometry of the cilium could be conferred by developmental constraints, interaction with associated proteins, or chemical differences between the A and B subfibers.

## DISCUSSION

Studies of the relationship between the structure and function of macromolecular complexes often rely on an ability to isolate parts of the complex through selective extraction. However, the extraction procedure must not alter the known properties of the complex if the results are to have any physiological rele-

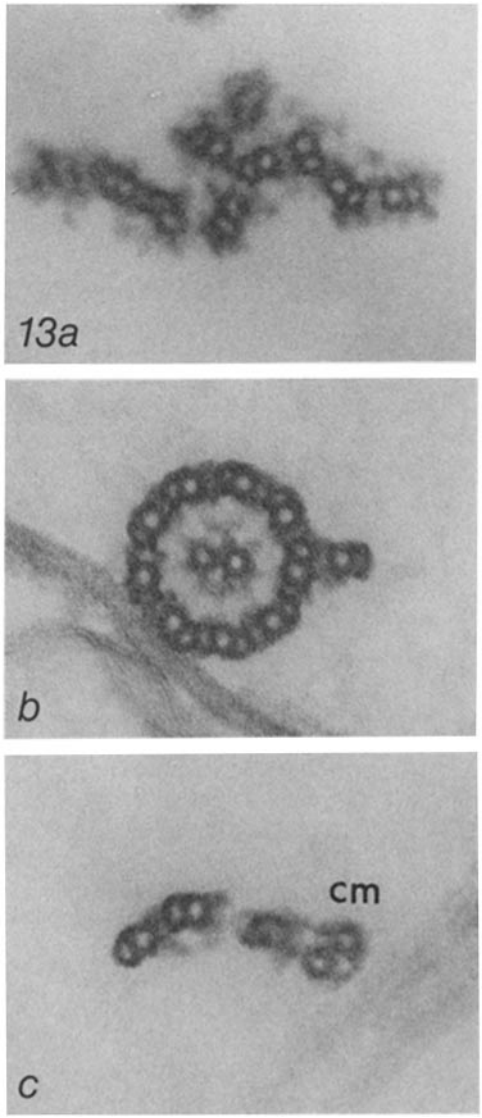


FIGURE 13 Electron micrographs of dynein-decorated doublets fixed in the presence of 6 mM $MgSO_4$. The arms interact with abnormal sites on outer-doublet microtubules (*a* and *b*) and central-pair (*cm*) microtubules (*c*). × 150,000.

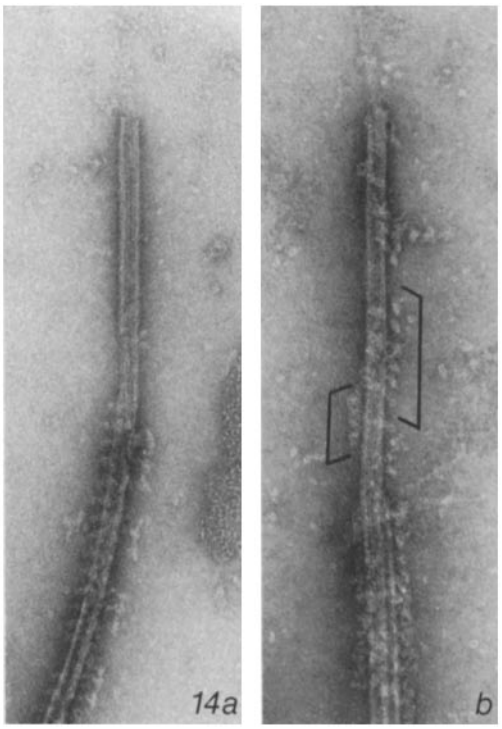


FIGURE 14 Electron micrographs of the distal tips of outer-doublet microtubules. (*a*) Doublet tip before dynein addition, showing the termination of radial spokes, dynein arms, and the B subfiber. (*b*) After the addition of dynein, arms project from both sides of the A tubule beyond the termination of the B subfiber (brackets) as well as decorating B-subfiber sites. × 100,000.

vance. The burden of proof lies with the investigator, and the best proof is the reconstruction of the complex to restore original function. Using sea urchin sperm flagella, Gibbons and Gibbons (7) have shown that dynein extracted into high salt solutions is capable of recombining with the extracted axonemes to restore normal beat frequency. In a similar fashion, we have shown that *Tetrahymena* dynein can be extracted by 0.55 M KCl and will rebind in a functional form. Fig. 2 demonstrates that rebound dynein arms retain the ability to attach at their proximal ends to A subfibers, to form cross-bridges to B subfibers, and to produce sliding forces when ATP is added. Force generation is itself a manifestation of two separate functions, ATPase activity, and mechanochemical coupling, both of which are restored by recombination. Other functions, such as the ability to respond to stimuli that modify active beat parameters, could also reside in the dynein arm complex. As other functions are defined, extraction and recombination will remain a powerful tool in localizing these functions to particular structural components of the axoneme. It is also hoped that the dynein arm complex can itself be fractionated into lesser components that retain subsets of the known dynein arm functions as suggested by the work of Hoshino (14–16), as this may aid in deciphering the role of individual peptides in the force-producing mechanism.

## Properties of Dynein Binding

Dynein arms must attach to the B subfiber in order for the energy of ATP hydrolysis to be converted into microtubule sliding. The dynein binding assay demonstrated in this study was designed to quantitatively examine the conditions that support dynein-B-subfiber interactions. This assay depends upon the change in turbidity (*A* 350 nm) measured when dynein binds to microtubules. The *A* 350 nm increases linearly with respect to the amount of protein (Fig. 5, top) or ATPase activity (Fig. 5, bottom) that binds. Absorbance measurements have the advantage of allowing the continuous monitoring of a sample during the consecutive addition of several test substances. In Fig. 6, the $Mg^{2+}$ dependence of the binding of isolated dynein to the exposed B subfiber of doublets is compared to the $Mg^{2+}$ dependence of *in situ* dynein arm cross-bridging taken from Zanetti et al. (39). There is a close correlation between dynein-B-tubule interactions as measured by these two methods. In both cases the interaction is highly $Mg^{2+}$ dependent and saturates at 3 mM $MgSO_4$.

The dissociation of dynein-B-subfiber interactions by ATP has been directly visualized by thin-section electron microscopy (36) and negative-contrast electron microscopy (31, and this paper). This ATP-induced release appears to represent a step in the cross-bridging cycle, the detachment which must occur if sliding is to proceed beyond the reach of a single dynein arm. In our initial attempts to quantitate this event we encountered two obstacles. First, decreases in *A* 350 nm were seen when no dynein had been bound and therefore did not reflect dynein release. These changes were traced to the secondary sliding of doublets that had reassociated during incubation in the presence of $Mg^{2+}$. The second obstacle was the apparent rapid depletion of ATP by hydrolysis, which decreased the effective nucleotide concentration when low concentrations of ATP were added (31). At ATP concentrations <200 μM, the drop in absorbance indicating dynein release is transient (no such transient phase occurs during sliding disintegration), and ATP may be hydrolyzed too rapidly for an accurate absorbance reading. No detailed analysis of this hypothesis has been made, but the inclusion of 10 μM vanadate, a 30S dynein ATPase inhibitor (18), completely eliminates the transient kinetics and the absorbance decrease remains stable. Vanadate also inhibits microtubule sliding (Fig. 9), but has no effect on the binding of dynein at a saturating $Mg^{2+}$ concentration (Fig. 10) or on the dissociation of dynein at a saturating $MgATP^{2-}$ concentration (Fig. 11).

Two previously reported phenomena that are also thought to depend on the maintenance of dynein cross-bridges show a similar sensitivity to low ATP concentrations. Flagella frozen into a rigor waveform by the rapid depletion of substrate will straighten in the presence of 1–3 μM $MgATP^{2-}$ (6); vanadate prevents the reactivation of rigor-wave flagella but does not inhibit the $MgATP^{2-}$ induced relaxation of the rigor waveform (8). The stiffness of demembranated flagella is also decreased by adding low concentrations of $MgATP^{2-}$ in the presence of vanadate (21), suggesting that bending resistance in the absence of ATP is maintained by dynein cross-bridges. Our direct observation that dynein arms are dissociated by micromolar ATP concentrations in the presence of vanadate supports the idea that dynein-B-subfiber interactions contribute to the bending resistance of flagellar axonemes and to the preservation of rigor waveforms in the absence of $MgATP^{2-}$. Conversely, the similarity between these phenomena observed in whole axonemes and our observations on the rebinding of isolated dynein argues that the rebinding and release of isolated dynein closely mimics *in situ* dynein-B-tubule interactions. It is somewhat surprising that attachment of the proximal ends of dynein arms to the A subfiber (or lack of attachment) has so little apparent effect on the interactions of the distal end with B-subfiber binding sites; the two ends appear to bind independently.

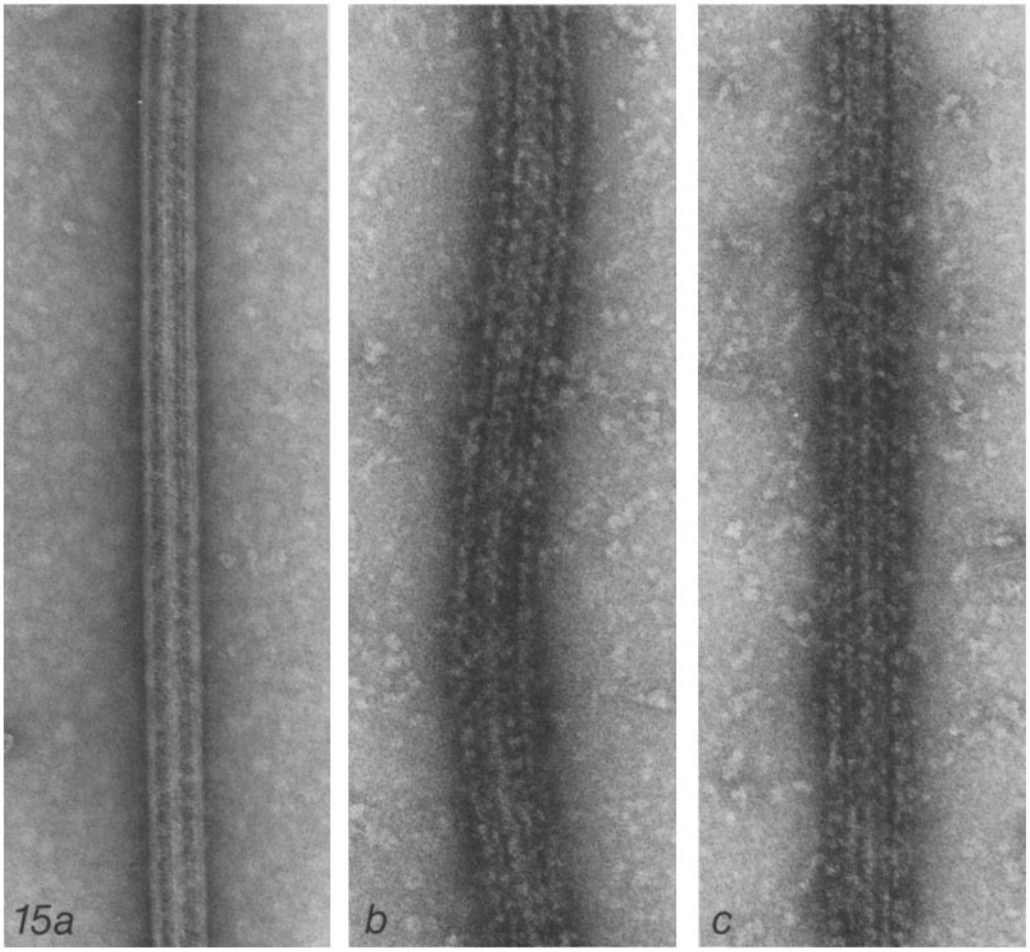


FIGURE 15 Electron micrographs of doublet microtubules negatively contrasted before (*a*) or after (*b* and *c*) the addition of a large excess of dynein. In *b* and *c* the doublets are decorated with several rows of arms. Each row is staggered with respect to the adjacent rows, producing a cross-hatched, 24-nm repeat pattern over the doublet microtubules (sight down the long axis). × 120,000.

TABLE I

*ATP-induced Inhibition of Dynein Binding to A and B Subfibers of Extracted and Unextracted Doublets in 10 μM Vanadate*

| | Extracted doublets | | Unextracted doublets | |
|---|---|---|---|---|
| exp | a | b | a | b |
| | | % | | |
| 1 | 37.0 | — | 54.3 | — |
| 2 | 18.9 | 12.6 | 78.0 | 74.0 |
| 3 | 37.2 | 37.2 | 83.7 | 58.7 |
| Mean | 31.0 | 24.9 | 72.0 | 66.4 |

Dynein binding under two conditions was measured from the increase in *A* 350 nm resulting when 30S dynein was added to a suspension of extracted or unextracted doublets. In condition *a*, 20 μM ATP was added 5 min after the addition of dynein, while in condition *b*, 20 μM ATP was added just before the addition of dynein. The two conditions show that dynein release (*a*) and inhibition of binding (*b*) are equivalent phenomena relative to classes of binding sites and the presence of ATP. Binding to extracted doublets is only ~30% inhibited by ATP, indicating the presence of predominantly ATP-insensitive (A-subfiber) binding sites. Binding to unextracted doublets is ~70% inhibited, indicating the presence of predominantly ATP-sensitive (B-subfiber) binding sites. Each value is the mean of two to five measurements.

A previous study in which ATP-induced decreases in turbidity were equated with the dissociation of dynein (31) may actually have recorded the drop in turbidity which accompanies the disintegration of trypsin-digested axonemes (26, 30, 38). *Tetrahymena* axonemes spontaneously disintegrate when exposed to $MgATP^{2-}$ without prior trypsin treatment as noted previously (37) and shown in Fig. 3. This disintegration is not seen in the presence of vanadate (Fig. 9) nor can it be induced by the nonhydrolyzable ATP analog adenylyl imidodiphosphate (AMP·PNP). Sea urchin axonemes will also disintegrate in $MgATP^{2-}$ but only if they are first incubated for a short time in trypsin (30). After prolonged trypsin treatment, axonemes are susceptible to a form of disintegration in which doublets separate from one another but do not slide (26). This form of disintegration is not dependent upon dynein mechanochemistry and hence will occur even when $MgATP^{2-}$ is added in the presence of vanadate (26). Two recent reports by Takahashi and Tonomura (31, 32) have used turbidity changes as an indication of dynein release from the B subfiber of *Tetrahymena* axonemes. Trypsin-treated axonemes were exposed to $MgATP^{2-}$ and the decrease in *A* 350 nm was used as a measure of dynein dissociation from the B subfiber. No quantitative relationship was established between the extent of dynein dissociation and the extent of the turbidity decreases. On the basis of our own results and those of Sale and Gibbons (26), it is difficult not to conclude that a considerable proportion of the absorbance changes recorded by Takahashi and Tonomura was the result of either active sliding disintegration or of the fraying mode of disintegration described by Sale and Gibbons.

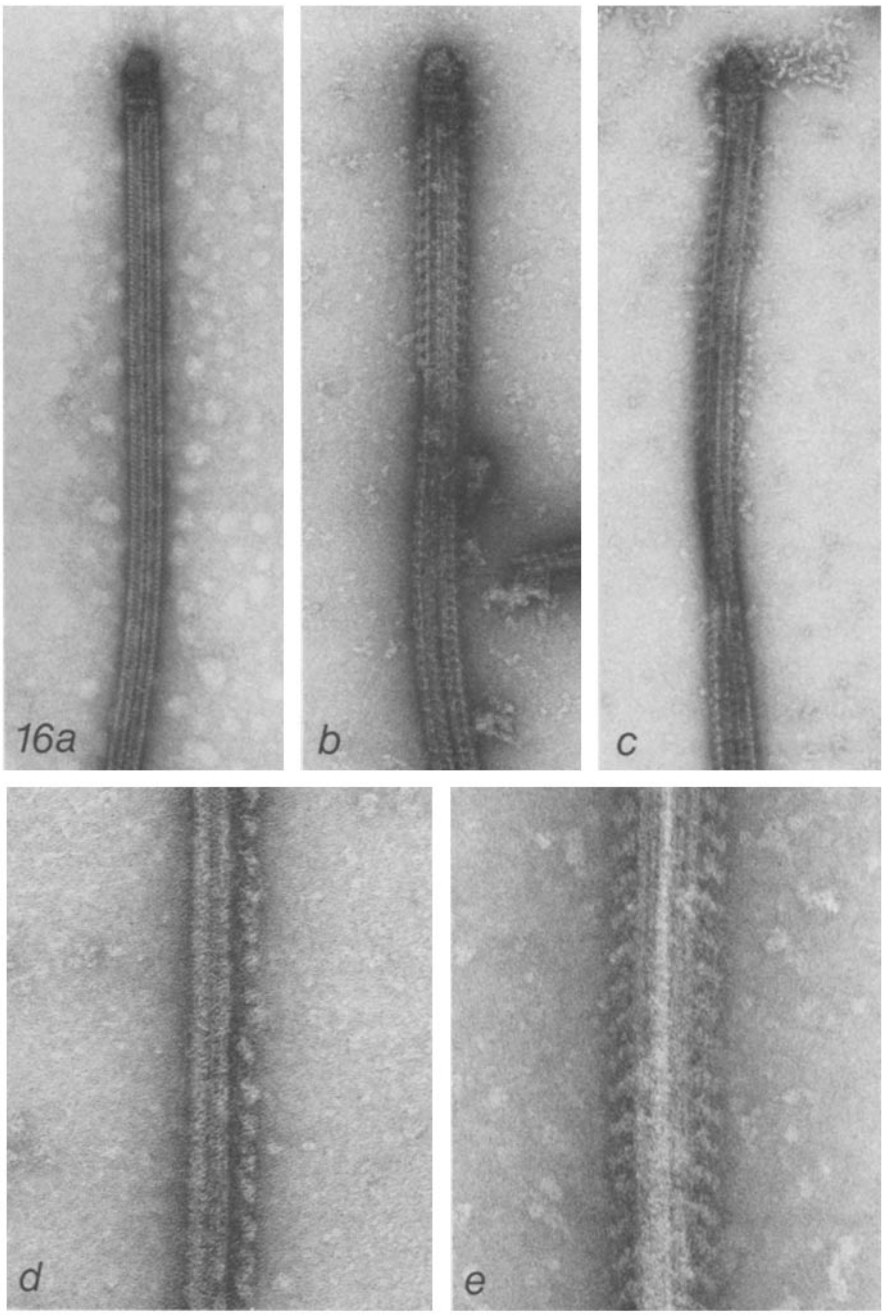


FIGURE 16 Electron micrographs of negatively contrasted central-pair microtubules. The normal appearance of the central-pair tip before dynein addition is shown in *a*. Added dynein binds only to the projection-free region, repeating at 24 nm and tilted towards the axoneme base (*b*–*e*). Dynein remains bound after the addition of 20 μM ATP (*b*–*e*). In *d* dynein has bound to one central-pair microtubule after the sheath projections were lost during isolation. *a*–*c* × 85,000. *d* and *e* × 180,000.

## *Binding Site Specificity*

Dynein arms *in situ* interact with two specific tubule sites; the proximal ends remain fastened in two rows to the A subfiber and the distal ends undergo cyclic attachment to specific sites on the opposing wall of the B subfiber. Because isolated dynein will form bridges between doublets in many abnormal positions and will also cross-link neurotubules, both ends of the arm are capable of binding to sites on the tubulin lattice and do not require the presence of nontubulin components or special classes of tubulin, although the existence of specialized binding sites may increase the specificity and stability of the attachment. Recombination of dynein with extracted axonemes shows that dynein will preferentially form proximal attachments to normal A-subfiber sites, and when these are not available, will attach proximally to nonspecific sites on A subfibers and central-pair tubules. B-subfiber sites appear to favor distal attachment because over half of the arms which attach to B subfibers can be dissociated by ATP.

An additional source of specificity may arise from cooperative interactions between adjacent binding sites on microtubules. Images of decorated tubules rarely show widely spaced individual arms, but rather patches of decoration and patches free from decoration (Fig. 17). A similar phenomenon was noted for neurotubule decoration (13), from which it appears that attachment of dynein to one site may favor the binding of additional arms with the same polarity to adjacent sites.

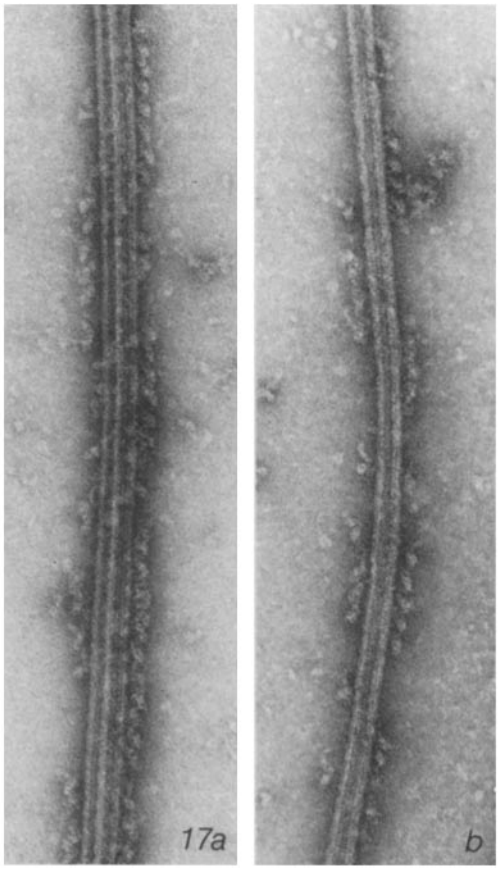


FIGURE 17 Electron micrographs of microtubules decorated with 30S dynein and negatively contrasted with uranyl acetate. At below optimal dynein concentrations, arms are often seen in discontinuous patches. (*a*) Extracted outer-doublet microtubule. (*b*) Projection-free central-pair microtubule. × 120,000.

## *Effects of Vanadate on Dynein Mechanochemistry*

Because dynein enzyme kinetics remain virtually unexplored, little is known about the kinetic mechanism and even less about the way in which vanadate interacts with the enzyme. Studies on the mechanism of vanadate inhibition of phosphatases indicate that vanadate may exist in a chelate form that resembles the transition state intermediate of phosphate hydrolysis (5, 35). Vanadate and inorganic phosphate both compete with ATP at the active site of Na, K-ATPase (5). In the case of dynein, vanadate produces an uncompetitive inhibition pattern (11, 18). This suggests that vanadate does not bind to the free enzyme form, which would result in competitive inhibition, but rather it must bind to an enzyme-substrate or enzyme-product complex. If vanadate binds by mimicking the transition state intermediate of the terminal phosphate of ATP, then it would not be expected to bind to E-ATP or E-P enzyme forms, as that site would be occupied. It could, however, bind to E-ADP to form an E-ADP-V complex. This would be consistent with a kinetic mechanism in which product release was sequential and ordered, and in which $P_i$ was released before ADP. If ADP is indeed the last product released, then it should be a competitive inhibitor of dynein ATPase activity. No kinetic studies on the inhibition of dynein have been made, but Okuno and Brokaw (22) report that $MgADP^-$ is a competitive inhibitor of the beat frequency of reactivated sperm flagella, Ki = 0.4 mM. Contradictory reports have appeared regarding the effects of inorganic phosphate on dynein ATPase activity. Under one set of conditions $P_i$ in concentrations up to 100 mM had no effects on 30S dynein ATPase activity (29), while under different conditions it is reported to be a weak inhibitor of whole axonemal ATPase activity (23). Okuno and Brokaw (22) find that $P_i$ is a weakly competitive inhibitor of whole axonemal beat frequency ($K_i$ = 60 mM), but as axonemes contain several ATPases whose activity may be essential for motility (12), it is difficult to determine the significance of this result to the dynein ATPase mechanism. Our results indicate that vanadate has no inhibitory effect on the release of dynein by ATP and are consistent with a mechanism in which vanadate does not compete with ATP for the free enzyme.

Models previously proposed for the dynein cross-bridging cycle (26, 31) have relied heavily on models of actin-myosin interactions. There are many similarities between actin-myosin and tubulin-dynein mechanochemistry, but there are many differences as well. In both cases the likely substrate is the $MgATP^{2-}$ complex, but isolated myosin is stimulated by $Ca^{2+}$ and inhibited by $Mg^{2+}$ (4), whereas dynein is inhibited by $Ca^{2+}$ and is insensitive to excess free $Mg^{2+}$ (14). Substrate binding appears to have similar effects in both systems. Kinetic studies show that $MgATP^{2-}$ binding lowers the affinity of myosin S1 for F-actin (19) and of 30S dynein for tubulin (14). Substrate binding can be mimicked by nonhydrolyzable analogues such as adenylyl imidodiphosphate (AMP-PNP) which induces a similar relaxation in muscle (20) and in rigor-wave sperm (24). The vanadate inhibition kinetics differ, however, actin-myosin giving a noncompetitive pattern at 37°C (18) while dynein produces an uncompetitive pattern at both 37°C (18) and 25°C (11). Trentham et al. (34) have shown that $P_i$ is a poor inhibitor of myosin MgATPase. $P_i$ binds slightly better to myosin than to myosin-ADP (2). If vanadate interacts in a manner similar to $P_i$, this would explain both the low sensitivity of myosin to vanadate and the noncompetitive inhibition pattern. The much greater sensitivity of dynein to vanadate, and the uncompetitive pattern which this inhibitor produces suggests a strictly sequential mechanism in which vanadate (and $P_i$) binds very poorly to the free enzyme but combines readily with an E-ADP intermediate. Vanadate + ATP may cause the accumulation of E-ADP-V intermediates with low affinity for tubulin, while vanadate + ADP is unable to back up the reaction mechanism to produce the same intermediate forms, as the addition of vanadate + ADP does not induce relaxation in sea urchin sperm (21). A more detailed correlation between the mechanical cross-bridging cycle and the enzymatic mechanism must await the results of further experimentation.

The kinetic mechanism discussed above is merely the simplest possible mechanism which is consistent with the currently available data; considerable modification of this scheme will be necessary as more information becomes available. It is hoped that this discussion may help to guide the direction of future research on kinetic models so that the known properties of dynein will be given greater consideration.

In conclusion, *Tetrahymena* 30S dynein extracted by 0.55 M KCl retains all of the known properties associated with the function of dynein arms in the intact axoneme. The binding of isolated dynein to B subfibers and its dissociation by ATP follow a pattern that is quantitatively similar to that of dynein arms *in situ*, suggesting that this system may provide a useful method for examining dynein-microtubule interactions in a quantitative fashion. The use of this assay, coupled with elec-

tron microscopy, has shown that both ends of the dynein arm are capable of making independent attachments to microtubules, but that attachment by the proximal end is endowed with greater stability and less specificity than is attachment by the distal end. 30S dynein binds preferentially to B-subfiber tubulin, but is also capable of interacting with other tubulin classes. The association constant for the dynein-tubulin interaction is increased severalfold by $Mg^{2+}$, although the exact nature of the $Mg^{2+}$ participation in this effect is not known. Conversely, ATP addition decreases the dynein-tubulin association through the formation of enzyme-substrate or enzyme-product intermediates with lowered affinity for tubulin. The major reaction intermediates that accumulate in the presence of vanadate are also low affinity forms. The fact that vanadate does not inhibit $Mg^{2+}$-induced binding or ATP-induced release of dynein is consistent with the uncompetitive nature of vanadate inhibition kinetics, and it is suggested that vanadate may form a dead-end complex with an E-ADP enzyme intermediate. A simple ordered sequential mechanism is presented that accounts for the known properties of vanadate action.

This study has been supported by research grant GM20690 from the National Institutes of Health.

*Received for publication 15 May 1980, and in revised form 27 June 1980.*

## REFERENCES

1. Amos, L. A., and A. Klug. 1974. Arrangement of subunits in flagellar microtubules. *J. Cell Sci.* 14:523–549.
2. Bagshaw, C. R., and D. R. Trentham. 1974. The characterization of myosin-product complexes and of product-release steps during the magnesium ion-dependent adenosine triphosphatase reaction. *Biochem. J.* 141:331–349.
3. Bradford, M. M. 1976. A rapid and sensitive method for the quantitation of microgram quantities of protein utilizing the principle of protein-dye binding. *Anal. Biochem.* 72:248–255.
4. Briggs, F. N., and R. J. Solaro. 1976. The role of divalent metals in the contraction of muscle fibers. *In* Metal Ions in Biological Systems. Vol. 6. H. Sigel, editor. Marcel Dekker, Inc., New York. 323–398.
5. Cantley, L. C., L. G. Cantley, and L. Josephson. 1978. A characterization of vanadate interactions with the (Na,K)-ATPase. *J. Biol. Chem.* 253:7361–7368.
6. Gibbons, B. H., and I. R. Gibbons. 1974. Properties of flagellar "rigor waves" formed by abrupt removal of adenosine triphosphate from actively swimming sea urchin sperm. *J. Cell Biol.* 63:970–985.
7. Gibbons, B. H., and I. R. Gibbons. 1976. Functional recombination of dynein I with demembranated sea urchin sperm partially extracted with KCl. *Biochem. Biophys. Res. Commun.* 73:1–6.
8. Gibbons, B. H., and I. R. Gibbons. 1978. Formation of flagellar rigor waves by abrupt removal of $Mg^{2+}$ from actively swimming sea urchin sperm, and the lack of inhibition by vanadate of the relaxation of rigor waves by MgATP. *J. Cell Biol.* 79:285*a*.
9. Gibbons, I. R. 1963. Studies on the protein components of cilia from *Tetrahymena pyriformis*. *Proc. Natl. Acad. Sci. U.S.A.* 50:1002–1010.
10. Gibbons, I. R. 1965. Chemical dissection of cilia. *Arch. Biol.* 76:317–352.
11. Gibbons, I. R., M. P. Cosson, J. A. Evans, B. H. Gibbons, B. Houck, K. H. Martinson, W. S. Sale, and W-J. Y. Tang. 1978. Potent inhibition of dynein adenosine triphosphatase and of the motility of cilia and sperm flagella by vanadate. *Proc. Natl. Acad. Sci. U. S. A.* 75:2220–2224.
12. Gibbons, I. R., E. Fronk, B. H. Gibbons, and K. Ogawa. 1976. Multiple forms of dynein in sea urchin sperm flagella. *In* Cell Motility. Vol. C. R. Goldman, T. Pollard, and J. Rosenbaum, eds. Cold Spring Harbor Laboratory. Cold Spring Harbor, New York. 915–932.
13. Haimo, L. T., B. R. Telzer, and J. L. Rosenbaum. 1979. Dynein binds to and crossbridges cytoplasmic microtubules. *Proc. Natl. Acad. Sci. U. S. A.* 76:5759–5763.
14. Hoshino, M. 1974. Preparation and characterization of a dissociated 14S form from 30S dynein of *Tetrahymena* cilia. *Biochim. Biophys. Acta.* 351:142–154.
15. Hoshino, M. 1975. Dissociation of *Tetrahymena* 30S dynein into 14S subunit by sonication. *Biochim. Biophys. Acta.* 403:544–553.
16. Hoshino, M. 1977. Tryptic fragmentation of 30S dynein from *Tetrahymena* cilia. *Biochim. Biophys. Acta.* 492:70–82.
17. Kepert, D. L. 1972. The Early Transition Metals. Academic Press, Inc., New York.
18. Kobayashi, T., T. Martensen, J. Nath, and M. Flavin. 1978. Inhibition of dynein ATPase by vanadate, and its possible use as a probe for the role of dynein in cytoplasmic motility. *Biochem. Biophys. Res. Commun.* 81:1313–1318.
19. Lymn, R. W., and E. W. Taylor. 1971. Mechanism of adenosine triphosphate hydrolysis by actomyosin. *Biochemistry.* 10:4617–4624.
20. Marston, S. B., C. D. Rodger, and R. T. Tregear. 1976. Changes in crossbridges when $\beta,\gamma$-imido-ATP binds to myosin. *J. Mol. Biol.* 104:263–276.
21. Okuno, M. 1980. Inhibition and relaxation of sea urchin sperm flagella by vanadate. *J. Cell Biol.* 85:712–725.
22. Okuno, M., and C. J. Brokaw. 1979. Inhibition of movement of triton-demembranated sea-urchin sperm flagella by $Mg^{2+}$, $ATP^{4-}$, ADP and $P_i$. *J. Cell Sci.* 38:105–123.
23. Otokawa, M. 1973. Inhibitory effect of inorganic phosphate on the axonemal ATPase of cilia from *Tetrahymena pyriformis*. *Biochim. Biophys. Acta.* 292:834–836.
24. Penningroth, S. M., and G. B. Witman. 1978. Effects of adenylyl imidodiphosphate, a nonhydrolyzable adenosine triphosphate analog, on reactivated and rigor wave sea urchin sperm. *J. Cell Biol.* 79:827–832.
25. Raff, E. C., and J. J. Blum. 1969. The fractionation of glycerinated cilia by adenosine triphosphate. *J. Biol. Chem.* 244:366–376.
26. Sale, W. S., and I. R. Gibbons. 1979. Study of the mechanism of vanadate inhibition of the dynein crossbridge cycle in sea urchin flagella. *J. Cell Biol.* 82:291–298.
27. Sale, W. S., and P. Satir. 1977. Direction of active sliding of microtubules in *Tetrahymena* cilia. *Proc. Natl. Acad. Sci. U. S. A.* 74:2045–2049.
28. Shimizu, T. 1975. Recombination of ciliary dynein of *Tetrahymena* with the outer fibers. *J. Biochem.* 78:41–49.
29. Shimizu, T., and I. Kimura. 1977. Effects of adenosine triphosphate on N-ethylmaleimide-induced modification of 30S dynein from *Tetrahymena* cilia. *J. Biochem.* 82:165–173.
30. Summers, K. E., and I. R. Gibbons. 1973. Effects of trypsin digestion on flagellar structures and their relationship to motility. *J. Cell Biol.* 58:618–629.
31. Takahashi, M., and Y. Tonomura. 1978. Binding of 30S dynein with the B-tubule of the outer doublet of axonemes from *Tetrahymena pyriformis* and adenosine triphosphate-induced dissociation of the complex. *J. Biochem.* 84:1339–1355.
32. Takahashi, M., and Y. Tonomura. 1979. Kinetic properties of dynein ATPase from *Tetrahymena pyriformis*. *J. Biochem.* 86:413–423.
33. Taussky, H. H., and E. Shorr. 1953. A microcolorimetric method for the determination of inorganic phosphorus. *J. Biol. Chem.* 202:675–685.
34. Trentham, D. R., R. G. Beardsley, J. F. Eccleston, and A. G. Weeds. 1972. Elementary processes of the magnesium ion-dependent adenosine triphosphatase activity of heavy meromyosin. *Biochem. J.* 126:635–644.
35. Van Etten, R. L., P. P. Waymack, and D. M. Rehkop. 1974. Transition metal ion inhibition of enzyme-catalyzed phosphate ester displacement reactions. *J. Am. Chem. Soc.* 96:6782–6785.
36. Warner, F. D. 1978. Cation-induced attachment of ciliary dynein crossbridges. *J. Cell Biol.* 78:R19–R26.
37. Warner, F. D., and D. R. Mitchell. 1978. Structural conformation of ciliary dynein arms and the generation of sliding forces in *Tetrahymena* cilia. *J. Cell Biol.* 76:261–277.
38. Warner, F. D., and N. C. Zanetti. 1980. Properties of microtubule sliding disintegration in isolated *Tetrahymena* cilia. *J. Cell Biol.* 86:436–445.
39. Zanetti, N. C., D. R. Mitchell, and F. D. Warner. 1979. Effects of divalent cations on dynein cross bridging and ciliary microtubule sliding. *J. Cell Biol.* 80:573–588.